



POLITECNICO DI TORINO  
Repository ISTITUZIONALE

Development of an innovative low-cost MARG sensors  
alignment and distortion compensation methodology

*Original*

Development of an innovative low-cost MARG sensors alignment and distortion compensation methodology for 3D scanning applications / Daniel Grivon; Enrico Vezzetti; Maria Grazia Violante. - In: ROBOTICS AND AUTONOMOUS SYSTEMS. - ISSN 0921-8890. - (2013), pp. 1710-1716. [10.1016/j.robot.2013.06.003]

*Availability:*

This version is available at: 11583/2511714 since: 2016-02-12T15:03:16Z

*Publisher:*

Elsevier

*Published*

DOI:10.1016/j.robot.2013.06.003

*Terms of use:*

openAccess

This article is made available under terms and conditions as specified in the corresponding bibliographic description in the repository

*Publisher copyright*

Elsevier postprint/Author's Accepted Manuscript

© 2013. This manuscript version is made available under the CC-BY-NC-ND 4.0 license  
<http://creativecommons.org/licenses/by-nc-nd/4.0/>. The final authenticated version is available online at:  
<http://dx.doi.org/10.1016/j.robot.2013.06.003>

(Article begins on next page)

# DEVELOPMENT OF AN INNOVATIVE LOW-COST MARG SENSORS ALIGNEMENT AND DISTORTION COMPENSATION METHODOLOGY FOR 3D SCANNING APPLICATIONS

**D. Grivon, E. Vezzetti, M. Violante**

*Dipartimento di Ingegneria Gestionale e della Produzione, Politecnico di Torino,  
Corso Duca degli Abruzzi 24, 10129, Torino, Italy  
Tel.: +39 011 5647294; Fax: +39 011 5647299; e-mail: [enrico.vezzetti@polito.it](mailto:enrico.vezzetti@polito.it)*

## **Abstract**

Working in the low cost 3D scanner design domain, it would be very interesting to employ inertial technologies because they could provide objects surface spatial data, recording they movement moving, and asking a very low cost in term of sensor investment. Unfortunately these technologies are characterised by distortion problems that normally do not allow to obtain satisfying measures for being employed for 3D scanning applications.

This situation happens working with Magnetic Angular Rate Gravity (MARG) sensor, on which many reports have been written to describe the methods used to suitably manage the data provided by the sensors in order to obtain an accurate orientation estimation, but only a few address the problem of calibration and distortion compensation. Furthermore, the proposed approaches usually involve both complex sensors models and accurate calibration facilities expensive from the workload, the computational and the economic points of view which compromise their possible employment in low-cost 3D scanning applications.

In this paper a novel approach for MARG sensors heading alignment and distortion compensation is proposed in order to increase the reliability of the information provided by the sensors and improve the process of attitude estimation, in order to get measurement quality level sufficient to be employable in 3D scanning applications.

Both the effectivity and the reliability of the proposed approach are validated by some experimental results and the performances are evaluated considering the quality of the outcome provided by the same attitude estimation algorithm processing raw data and compensated data.

**Keywords:** 3D Scanners, Magnetic Angular Rate Gravity, Calibration Procedure, Attitude Estimation.

## 1. INTRODUCTION

The need to obtain a 3D model, given a real object, a shape, or a surface, is becoming more and more important in different fields and for different purposes. For this reason, 3D scanner builder is investing in new technologies able to acquire the entire shape of complex object without constraints in term of object dimensions, locations, and material typologies. Accordingly, it is necessary to dispose of flexible tools that move around the object and allow to acquire the entire object shape without complex and time consuming software post processing operations. Some devices work employing special scanning heads with tracking systems for recording the head spatial position during the acquisition phase, while other employ special marker, located on the object surface, for maintaining fixed reference during the scanning tasks. All these technologies are able to provide interesting results, but are very expensive, so they could not be employable by all those people that could get advantages by the availability of 3D virtual model of real objects. Therefore, it is also

necessary to invest in other low technologies/sensors able to support the development of 3D scanning devices without important investments [1,2]

In recent years, the scope linked to the inertial navigation has seen the development of numerous research activities in transversal fields of applications, ranging from the dead reckoning to the assisted navigation, from the motion tracking to biomedical applications. This development was supported above all by new possibilities given by silicon manufacturing processes that led to the creation of specific sensors able to guarantee medium-high performance at reasonable prices. In this context, the measurement units known as **MARG** (**M**agnetic **A**ngular **R**ate **G**ravity, mounting on-board an accelerometer, a gyroscope, and a magnetometer) have been widely used and studied. Starting from real time motion tracking for virtual reality applications [3,4] till arriving to aerospace vehicles and satellites control [5,6] these sensors are able to provide significant added values to different application domains.

Their development and subsequent use arises from the need to mitigate estimation errors (mainly due to measurement noise or drift phenomena) that are generated in the process of integration of data provided by gyroscope (attitude determination) and accelerometer (position determination) necessary to obtain the overall information defining the position and orientation of a body.

More recently, many research activities have focused in identifying the best methods of processing the information provided by MARG only for determining the orientation of a device: Using Complementary Filter [7,8] or the Kalman Filter [9,10] are the two most commonly used solutions that, although different in their theoretical foundations and implementation strategies, plan to use the orientation information provided by accelerometer and magnetometer to support the data acquired by the gyro in order to correct the drifts and other errors.

In this context the growing trends towards modern 3D scanning systems, that include the use of a scanning head (equipped with a probe or with a laser scanner) free from physical constraints, imply the possibility to install a MARG measurements unit able to determine the orientation of scanning head itself. Anyway, this strategy implies that the attitude of the device can be computed, while the problem position determination is not solved yet.

On the contrary, in the case in which the information that define the orientation are directly used to obtain three-dimensional displacement of the scanning device itself, the relevance of a correct attitude determination is crucial. In particular, the authors have highlighted how, starting from data that define a 2D path laying on the plane always tangent to the acquiring surface, it is possible to obtain a three-dimensional tracking of the movement done (thus a correct reconstruction of the surface on which the device is slid) [11].

In this context, however, the accuracy degree required for the data that define the attitude of the scanning device is very high. In particular, it is necessary to underline how even small constant errors in the orientation estimation may lead to drift phenomena and to consequent unreliable scanning results.

In this sense it is fundamental to define an efficient and convenient procedure (from the workload, the computational and the economic points of views) for calibration and alignment of the various sensors mounted on the board in order to ensure the reliability of respective information as well as the coherence between data provided by different sensors.

In fact, although many publications on the methodology to manage data provided by MARG have been done and the problem of correct identification of the sources of error in such measurement units (such as measurement noise, drift of the sensors...) has been addressed in several ways, less interest has been devoted to the formulation of innovative and functional methods of calibration for low-cost inertial sensors in order to obtain good results without resorting to the use of complex equipment calibration or to elaborate sensor models [12]. Jurman et al. [13], referring to [14,15], treat directly the problems of calibration of MEMS sensors and the correction of defects due to manufacturing process or by misalignment during assembly of the board, providing anyway a complex calibration model that requires a considerable computational effort in the determination

of the 36 parameters that define the model itself. The majority of other authors do not consider as crucial the problem of an exact calibration, but prefer to include the distortions in the characteristic of the sensors, the phenomena of mutual misalignment or the incorrect scale factors within the system model used to determine the orientation of the device itself, increasing however the overall complexity of the estimation algorithm [10].

On the other hand, one of the few references dealing with specific problems of testing and calibration compensation [16] offers compensation and calibration routines making use of sophisticated and expensive equipment whose use should be to affect target low-cost considered in the choice initial components and targets of the project.

This paper presents an innovative and effective alternative to the mentioned solutions providing a simple routine, yet effective, for the calibration of low-cost sensors, the removal of offsets, the compensation of misalignment between mutual sensors and compensation of any non-linearity and distortion present in the sensors themselves for supporting the employment of MARG in 3D scanning applications.

## 2. PROPOSED METHODOLOGY

In the following section the methodology and the routines used to perform the *sensor plane alignment* and the *calibration & compensation routine* are proposed [17]. A sensor plane alignment methodology has been designed and developed with the aim to provide a simple, but at the same time effective, method that fixes the misalignment among the different sensors assuming a starting reference plane (in the following the reference plane is the XY plane of the board). The following chart (Fig.1) resumes well the four phases that compose the alignment routine.

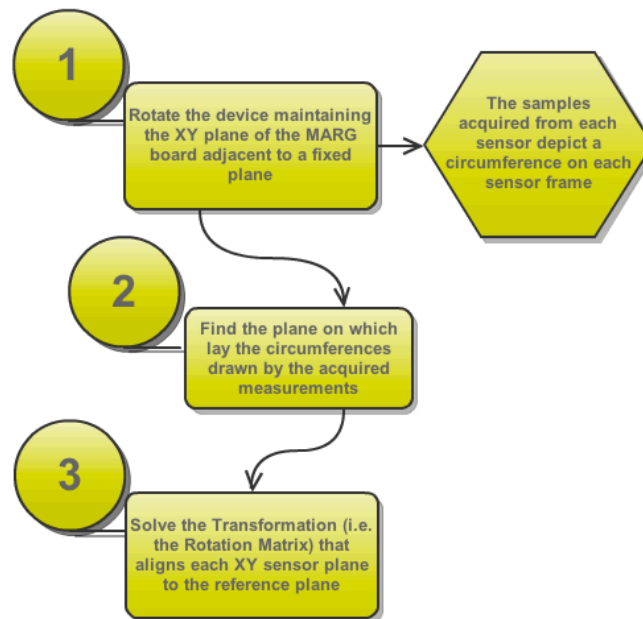


Figure 1: Main steps of Sensor Plane Alignment Routine.

As evident, the result of this routine is an *alignment matrix*: in order to remove the misalignment among the different sensor planes and obtain consistent data every next measurements have to be aligned (i.e. multiplied by the respective *alignment matrix*) according to relation founded.

Equally, the *calibration & compensation routine* can be defined using four main steps (Fig.2). Once the coefficients defining the ellipsoid features are found, each sample successively acquired must be correct performing the 4<sup>th</sup> step. Anyway, because of the last operation requires firstly to rotate the acquired sample and then to correct the axes gains, it is necessary to restore the initial orientation of the samples after the compensation is performed: this is done multiplying the compensated measurement by the inverse of the DCM matrix.

Although the *planes alignment* method and the *calibration & compensation routine* can be considered as two stand-alone processes, they must be both performed in succession in order to obtain an optimal result and provide a real increase in the reliability of the sensor measurements.

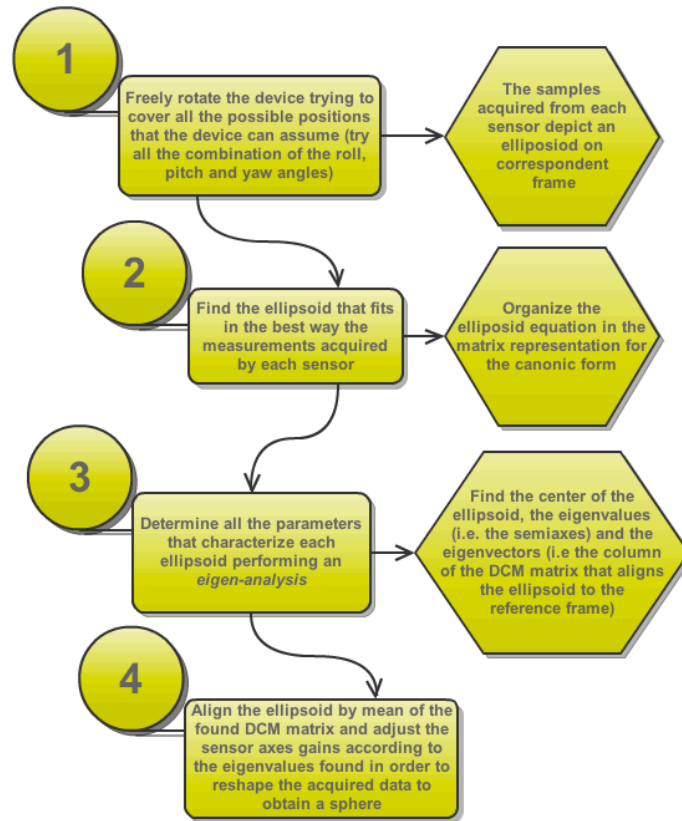


Figure 2: Main steps of Calibration & Compensation Routine.

### 2.1 Sensor Plane Alignment

If the device is rotated keeping this reference plane always lying on a fixed plane, then the vector of the corresponding physical quantity measured by each sensor (i.e. the gravity vector for the accelerometer and the magnetic vector for the electronic compass that remains fixed in the navigation frame), should depict a cone in the body reference system for each rotation of  $360^\circ$  (Fig.3). Considering an ideal situation in which the sensor planes are perfectly aligned to each other and to the reference, the axis of rotation must coincide with the axis of the cone, while the tip of the arrow that represents the physical quantity (i.e. the acceleration vector or the magnetic vector) must trace a circle that lies on a plane parallel to the rotation plane: this phenomena is related to the assumption of keeping the device always rotating on the same fixed plane, that constraints the z coordinate to have no variation.

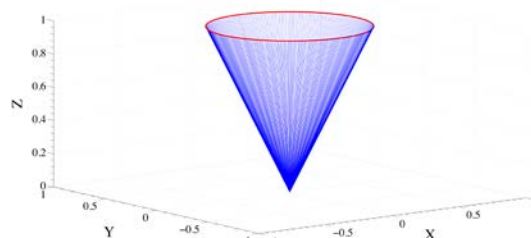


Figure 3: The ideal cone drawn by the physical vector in the body frame.

Due to the sensor misalignment, the data are deviated. The aim of the alignment procedure is to minimize this deviation. In order to evaluate the misalignment of each sensor, a complete rotation done by keeping the reference sensor plane coincident to a fixed plane is required. By this way every physical quantity measured by the correspondent sensor and represented as a vector will ideally draw a circle on the MARG body frame.

Once the data are collected it is possible to define the misaligned planes for each sensor as the planes that contain the different circumferences defining the bases of the cones drawn by the vector tips (Fig. 4).

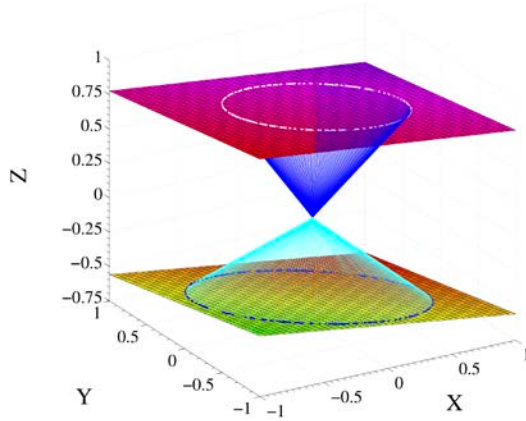


Figure 4: The cones drawn for the physical vectors and the misaligned planes containing the data.

In particular, the equation representing a plane can be written as

$$z = \alpha x + \beta y + \gamma, \quad (1)$$

where  $x, y, z$  represent the Cartesian variables in a three-dimensional space and  $\alpha, \beta, \gamma$  are the coefficients that defines the features of the plane. Furthermore, once a XY plane for each sensor is defined, a vector normal to each plane can be defined as

$$v_{norm} = [-\alpha, -\beta, \gamma]. \quad (2)$$

Figure 5 shows the circles of the collected data, the different planes, and the orthogonal vectors during an alignment session.

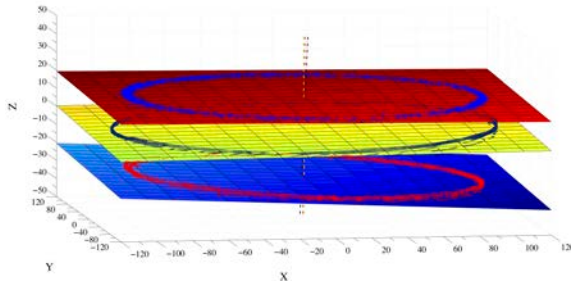


Figure 5: The circles drawn by the physical vectors sensed by the different sensors: the normal vectors of each planes are clearly visible.

The final step in the alignment routine is to define the two consequent rotations, the first of an angle  $\varepsilon_{Roll}$  around the  $x$  axis and the second of an angle  $\varepsilon_{Pitch}$  around the  $y$  axis, that align the normal vector of each plane to the normal vector of the reference plane, namely  $v_{norm.ref} = [0,0,1]$ .

The result of this calibration method is an alignment matrix for each sensor that has the well-known structure

$$M_{Align} = \begin{pmatrix} \cos \varepsilon_{Roll} & \sin \varepsilon_{Pitch} \sin \varepsilon_{Roll} & \cos \varepsilon_{Pitch} \sin \varepsilon_{Roll} \\ 0 & -\cos \varepsilon_{Pitch} & -\sin \varepsilon_{Pitch} \\ -\sin \varepsilon_{Roll} & \sin \varepsilon_{Pitch} \sin \varepsilon_{Roll} & \cos \varepsilon_{Pitch} \cos \varepsilon_{Roll} \end{pmatrix}. \quad (3)$$

Once the alignment matrices are obtained for all the sensors, it is possible to multiply each set of data for its corresponding rotation matrix (Fig.6).

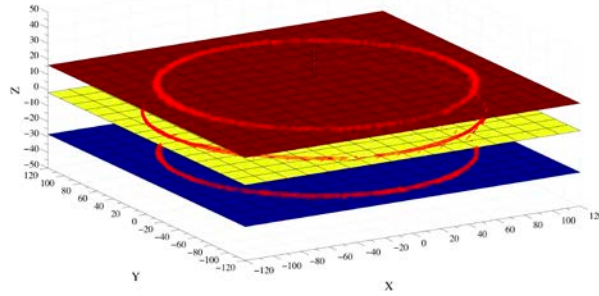


Figure 6: The aligned planes for the different sensors.

## 2.2 Calibration & Compensation (Offsets Removal, Nonlinearities and Distortions).

The *Offsets Removal, Nonlinearities and Distortions Compensation* methodology aims at fitting the 3D data drawn in each sensor reference frame by the physical vectors (sampled for an acquisition session during which the MARG board is freely rotated around its reference axes) with an ellipsoid, removing the offsets, centring the fitted ellipsoid, and finally correcting the gains for the sensor axis triads in order to reshape the data to obtain a sphere.

Since the following directly refers to topics of linear algebra, it seems appropriate to introduce the mathematical foundations used, in order to firstly clarify all the symbols used.

There are various representative forms for an ellipsoid [18,19,20]:

*Algebraic form:*

$$\Gamma(x, y, z) = Ax^2 + By^2 + Cz^2 + Dxy + Eyz + Fxz + Gx + Hy + Jz + K = 0, \quad (4)$$

where the terms  $A, B, C, D, E, G, H, J,$  and  $K$  are constants.

*Parametric form:*

$$\Gamma(x, y, z) = \begin{cases} x = a \cos \delta \cos v \\ y = b \cos \delta \sin v \\ z = c \sin \delta, \end{cases} \quad (5)$$

where  $0 < \delta \leq 2\pi$  and  $0 < v \leq \pi$ . A particular relevance assumes the *matrix form* that rearranges the *algebraic form* and describes the same ellipsoid as

$$\tilde{X}S\tilde{X}^T = 0, \quad (6)$$

where

$$\tilde{X} = [x, y, z, 1] \quad (7)$$

and

$$S = \frac{1}{2} \begin{pmatrix} 2A & D & F & G \\ D & 2B & E & H \\ F & E & 2C & J \\ G & H & J & 2K \end{pmatrix}. \quad (8)$$

The translation matrix of the ellipsoid centre from the origin to  $[X_c, Y_c, Z_c]$  is defined as

$$\begin{pmatrix} x - X_c \\ y - Y_c \\ z - Z_c \\ 1 \end{pmatrix} S \begin{pmatrix} x - X_c \\ y - Y_c \\ z - Z_c \\ 1 \end{pmatrix}^T = 0 \quad (9)$$

and can be accomplished by the matrix

$$T = \begin{pmatrix} 1 & 0 & 0 & 0 \\ 0 & 1 & 0 & 0 \\ 0 & 0 & 1 & 0 \\ -X_c & -Y_c & -Z_c & 1 \end{pmatrix}, \quad (10)$$

where

$$\tilde{X} \underbrace{TS^*T^T}_s \tilde{X}^T = 0. \quad (11)$$

Thus, once found the translation coordinates, it is possible to centre the ellipsoid in the origin and simplify the terms  $G, H, J$ . Then, by dividing all the achieved coefficients by the new constant term  $L$ , we finally obtain the canonical form of an ellipsoid that we will express, without abuse of notation, as

$$Y(x, y, z) = ax^2 + by^2 + cz^2 + 2dxy + 2eyz + 2fzx = 1. \quad (12)$$

The equivalent matrix representation is

$$Y(x, y, z) = (x \ y \ z) \begin{pmatrix} a & d & e \\ d & b & f \\ e & f & c \end{pmatrix} \begin{pmatrix} x \\ y \\ z \end{pmatrix} = 1, \quad (13)$$

where  $a, b, c, d, e,$  and  $f$  are constant and can be obtained as



$$a = -\frac{A}{L}; \quad b = -\frac{B}{L}; \quad c = -\frac{C}{L}; \quad (14)$$

$$d = -\frac{D}{2L}; \quad e = -\frac{E}{2L}; \quad f = -\frac{F}{2L}. \quad (15)$$

Now it is possible to find the direction of the three ellipsoid principle axes performing an algebraic Eigen analysis. The subject of Eigen analysis seeks to find a coordinate system, in which the solution to an applied problem has a simple expression. Therefore, Eigen analysis might be called the method of *simplifying coordinates*. An ellipsoid can be also defined as a geometric object described by its semi-axes. In the vector representation, the semi axes directions are unit vectors  $v_1, v_2, v_3$  and semi-axes lengths are constant  $a, b, c$ . The vectors  $av_1, bv_2, cv_3$  form an orthogonal triad. Algebra does not change the triad: the invariants  $av_1, bv_2, cv_3$  must somehow be hidden in the equations that represent the ellipsoid. Solving the Eigen problem for the matrix  $A$  means to find the eigenvectors (i.e. *the hidden vectors*)  $v_1, v_2, v_3$  and the eigenvalues (i.e. *the hidden values*)  $\lambda_1, \lambda_2, \lambda_3$  for the matrix  $A$  so that

$$A = RDR^T, \quad (16)$$

where  $R$  consists of three columns of mutually orthogonal unit eigenvectors and  $D$  is a diagonal matrix with the three eigenvalues along its diagonal. Thus, considering the previously introduced relations, we obtain

$$Y(x, y, z) = (x \ y \ z)RDR^T \begin{pmatrix} x \\ y \\ z \end{pmatrix} = (X \ Y \ Z)A \begin{pmatrix} X \\ Y \\ Z \end{pmatrix} = \lambda_1 X^2 + \lambda_2 Y^2 + \lambda_3 Z^2 = 1, \quad (17)$$

where the eigenvectors columns of  $R$  define a new rotated coordinate system  $X, Y, Z$ ; thus matrix

$$R = (v_1^T \ v_2^T \ v_3^T) \quad (18)$$

represents in all respects a rotation matrix, i.e. a *DCM matrix*, that aligns the coordinate system  $x, y, z$  to the new reference frame  $X, Y, Z$ . In the end, the last useful equation underlines the relation between eigenvectors and semi-axes resulting in the common ellipsoid expression

$$Y(x, y, z) = \frac{X^2}{a^2} + \frac{Y^2}{b^2} + \frac{Z^2}{c^2}, \quad (19)$$

according to which is clear the correspondence

$$a = \sqrt{\frac{1}{\lambda_1}}; \quad b = \sqrt{\frac{1}{\lambda_2}}; \quad c = \sqrt{\frac{1}{\lambda_3}}. \quad (20)$$

The following figure (Fig.7) shows how the data acquired by freely rotating the MARG board trying to cover all the possible orientation positions.

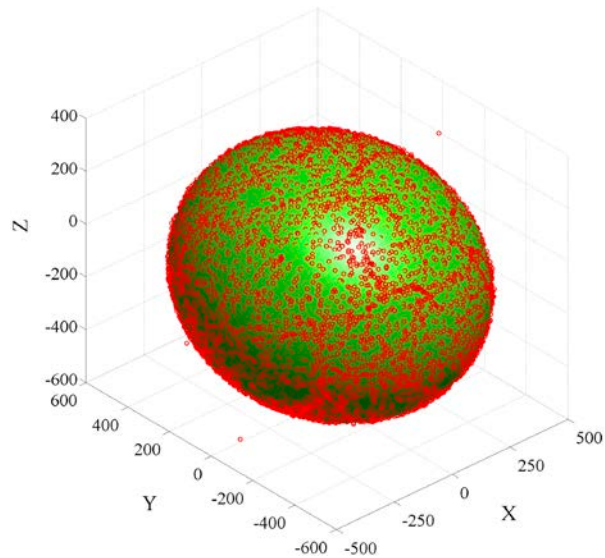


Figure 7: An example of the samples acquired by the magnetometer and the underlying ellipsoid obtained fitting the data.

As introduced, the geometrical surface drawn by the vector tip of the physical quantity measured (in this case it is the magnetic field samples are shown by red dots) in the several orientations is an ellipsoid. The underlying mesh represents the best ellipsoid that fits the data and from which the *Eigen analysis* is performed.

In the following figure (Fig.8) it is possible to have a quick confrontation between the raw uncalibrated magnetometer measurements (blue dots) and the data after the compensation process (red dots). It can be easily observed that the proposed method removes the distortions on the sensor model and compensate the presence nearby magnetic sources. In fact, the compensated data describe a surface that approximates very well the ideal case in which the acquired unbiased and undistorted sample should depict a sphere.

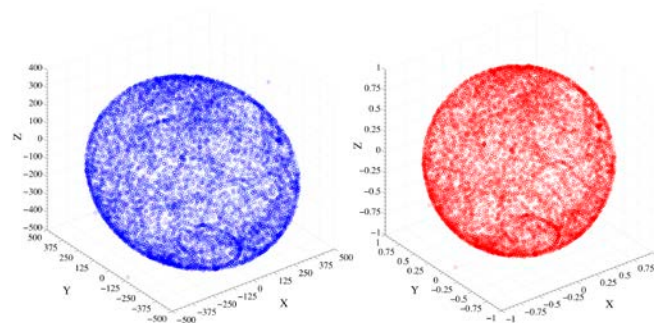


Figure 8: The raw magnetometer measurements (blue dots) and the same data obtained after the compensation routine described beforehand (red dots).

### 3. EXPERIMENTAL VALIDATION

The measurements unit used is a low-cost tool that embeds a 3 axes gyroscope ITG-3200 produced by InvenSense which guarantees a sensitivity of 14,375 LSB/(°/s) and low total RMS noise (about 0.35 RMS), a 3 axes accelerometer ADXL345 produced by Analogue Devices with a good resolution of 3,9 mg/LSB and an adequate bandwidth of 3.2 KHz, a digital compass (magnetometer) HMC 5883L with a good sensitivity of 0.73 mGauss/LSB which enables 1° to 2° compass heading accuracy. The codes for processing the acquired data are run on a general purposes computer.

In order to evaluate the results of the different phases of the proposed method, the *raw* samples, the *compensated* data, and the *aligned-compensated* data provided by the accelerometer and the magnetometer are elaborated using the Gauss-Newton Method [21] for quaternion convergence discussed in [11]. In particular, this method, which is used to solve the nonlinear problem in the quaternion components that transforms the reference physical quantities in a fixed frame (i.e. the Earth reference frame) in the sampled quantities that result to be rotated in accordance to the MARG board orientation, quickly converges to the solution with respect to other nonlinear solution approaches used as Quaternion Estimation algorithm as the *Gradient Descent algorithm* [22] or the *Newton Method* [23].

The movement performed during this test session requires that the XY plane of the board has to be kept always in contact and laying on a reference inclined plane; by rotating the device around its Z axis, the measurements obtained in ideal conditions (absence of distortions, noise, and perfect alignment of all the sensors) should depict no change for the *roll* and the *pitch* angles and more than  $360^\circ$  (a rotation) for the *yaw* angle. Thus, the quality of the method can be evaluated as the value the *roll* and *pitch* angles assume (i.e. the difference from the ideal value of  $0^\circ$ ). Figure 9 shows the angles solved by this algorithm and allows to focus on the different improvements provided by each step of the *alignment/compensation* process.

Furthermore, it must be considered that the measurements provided by the accelerometer and the magnetometer are really noisy and any filter is actually applied.

The blue lines represent the angles obtained using the *misaligned and distorted* measurements: it is evident how the raw samples produce unreliable angles. Besides, it is evident how the proposed methods act on the raw data improving their quality; the *compensation routine* is able to reduce the highest peaks in the angles detection, while it maintains the deviation due to the sensor plane misalignment. The *alignment method* finally fixes also this aspect and provide values for the roll and the pitch angles really close to the ideal situation.

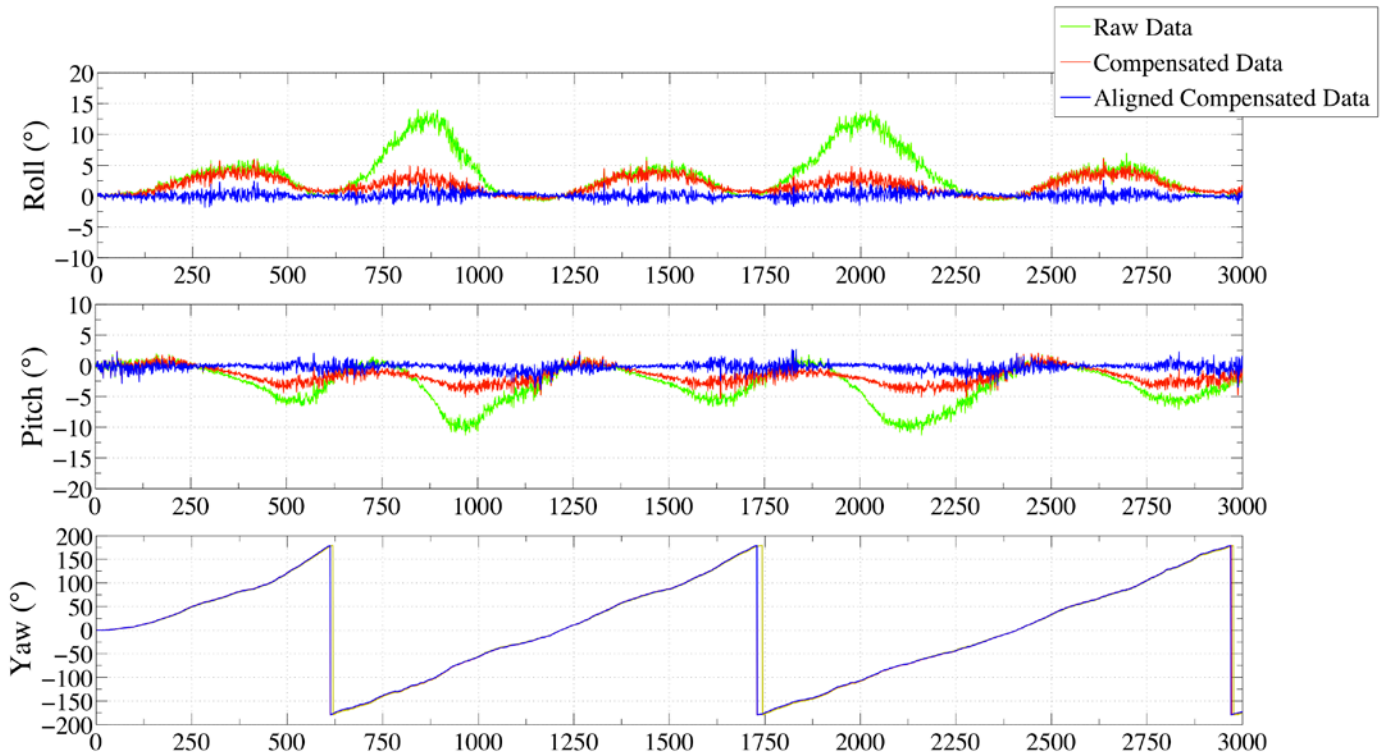


Figure 9: The roll, pitch and yaw angles solved by the Gauss-Newton algorithm.

Another mean to evaluate the quality of the proposed routine is the *Objective Function* (or *Cost Function*) of the Gauss-Newton Method. In fact, considering that the *Cost Function* describes the trend in the convergence of the Gauss-Newton algorithm, it is obvious that high values of  $F(x)$  imply non-consistent and incompatible information provided by the different sensors and, thus, an unreliable attitude estimation.

In this sense, the low values assumed in the case of using compensated data for quaternions estimation is another index of the high quality of the *alignment-compensation* routine performed that produces a reduction of more than one order of magnitude in the mean value of  $F(x)$ (Tab.1).

	Cost Function $F(x)$
Raw Data	$8,539 \cdot 10^{-4}$
Compensated Data	$1,096 \cdot 10^{-4}$
Aligned-Compensated Data	$2,231 \cdot 10^{-5}$

Table 1: Cost Function Values.

In fact, the high values of  $F(x)$  for the misaligned and uncompensated data (green plot) underline how the consistency of the information given by the sensors is really low: this aspects results in the bad attitude estimation shown by the green plot in figure 9.

The major improvement in the orientation estimation is given by the compensation routine: in fact, the distortions that affect above all the magnetometer, but also the other sensors, produce the largest error and result in the highest peak in the *roll* and *pitch* angles. Consequently, after the compensation is applied, the consistency of the different information increases and the mean and the maximum values of  $F(x)$  actually decrease (red line).

Finally, the alignment routine further improves the overall quality of the sample: the *roll* and *pitch* angles drawn by the blue plot in figure 10 are really near to the ideal reference of  $0^\circ$  (the mean error is about  $0.32^\circ$ ) and the value of the *Cost Function* is reduced of more than one degree of magnitude with respect to the values shown with raw data.

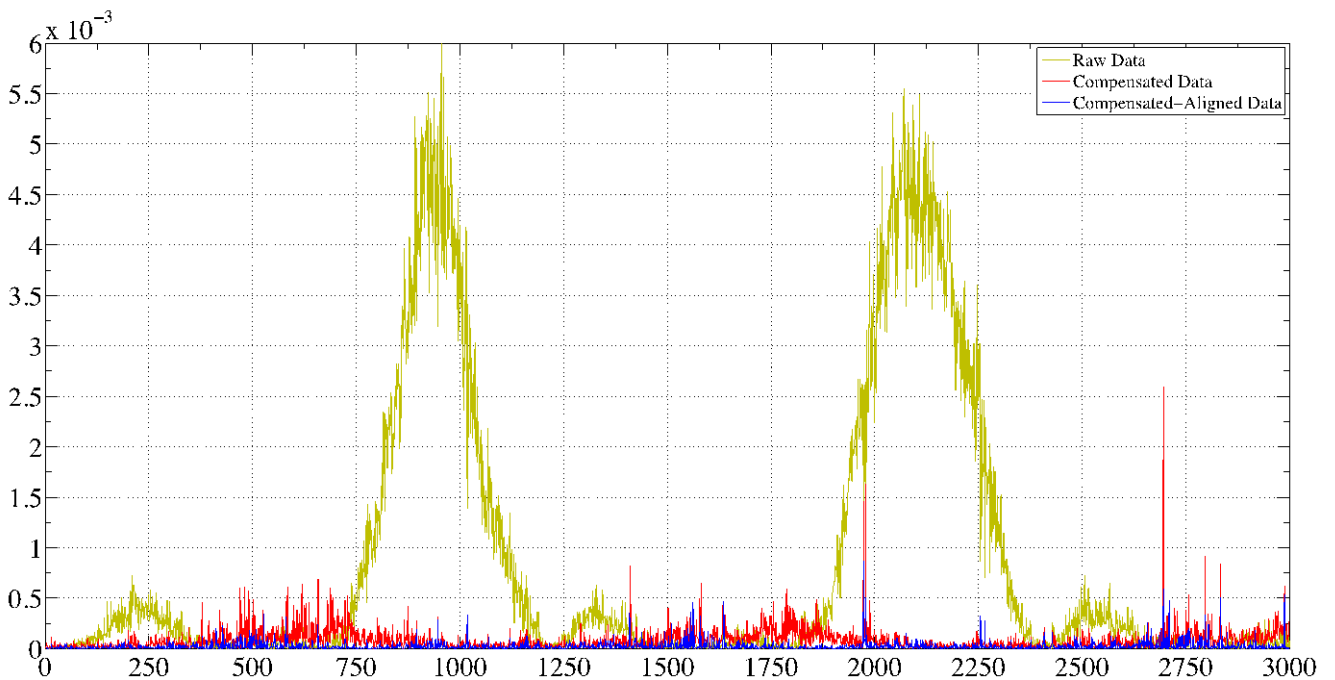


Figure 10: The Objective Function of the Gauss-Newton algorithm for the different sets of data

#### 4. CONCLUSION

This paper discusses a novel method for calibration, sensor plane alignment and distortions compensation of low cost MARG platform. After a detailed overview of the theoretical aspects involved in the routine, the method is presented in its *easy-to-use* nature, which complies with the low cost nature of the sensors considered. The results clearly underline the quality and the reliability of the proposed approaches that are able to improve the quality of inertial and magnetic measurements and solve the problems related to nonlinearities and distortions.

The benefits of this method result even more evident if we consider the reduction of further workload required to implement complex sensor model that takes into account the nonlinearities that lay in the sensors.

#### 5. REFERENCES

- [1] E. Vezzetti, "Optimal pitch map generation for scanning pitch design in selective sampling", *Robotics and Autonomous Systems*, Vol.57, No.6 – 7, pp. 578 – 590, 2009
- [2] E. Vezzetti, "Computer Aided Inspection: design of customer oriented benchmark for non contact 3D scanners evaluation", *International Journal of Advanced Manufacturing Technology* Vol.41, No.11-12, pp. 1140 – 1151, 2009
- [3] Z. Rong, "A real-time articulated human motion tracking using tri-axis inertial/magnetic sensors package", *IEEE Transaction on Neural Systems and Rehabilitation Engineering* Vol.12, No.2, pp. 295 – 302, 2004
- [4] E. Banchmann, "Inertial and magnetic posture tracking for inserting humans into networked virtual environments", *Proceedings of the ACM symposium on Virtual reality software and technology*, pp. 9 – 16, 2001
- [5] E. Silani, M. Lovera, "Magnetic spacecraft attitude control: a survey and some new results", *International Journal of Control Engineering Practice*, Vol.13, No. 3, pp. 357 – 371, 2005
- [6] A. Astolfi, M. Lovera, "Global magnetic attitude control of spacecraft in the presence of gravity gradient", *IEEE Transaction on Aerospace and Electronic Systems*, Vol.42, No. 3, pp. 796 – 805, 2006
- [7] M. Euston, P. Coote, R. Mahony, J. Kim and T. Hamel, "A Complementary Filter for Attitude Estimation of a Fixed-Wing UAV".
- [8] R. Mahony, T. Hamel and J. M. Pflimlin, "Nonlinear Complementary Filters on the Special Orthogonal Group", *IEEE Transaction on Automatic Control*, Vol. 53, No. 5 , pp. 1203-1218.
- [9] D. Gebre-Egziabher, G. H. Elkaim, J. D. Powell and B. W. Parkinson, "A Gyro-Free Quaternion-Based Attitude Determination System Suitable for Implementation Using Low Cost Sensors", *Position Location and Navigation Symposium*, IEEE 2000, pp. 185-192.
- [10] A. Sabatini, "Quaternion-Based Extended Kalman Filter for Determining the Orientation by Inertial and Magnetic Sensing", *IEEE Transactions on Biomedical Engineering*, Vol. 52, No. 7, July 2006.

- [11] D. Grivon and E. Vezzetti, "Study and Development of a low-cost OptInertial 3D Scanner", In Press
- [12] M. S. Grewal, "Application of Kalman Filtering to the Calibration and Alignment of Inertial Navigation Systems", IEEE Transactions on Automatic Control, Vol. 36, No. 1, January 1991
- [13] D. Jurman, M. Jankovec, R. Kamnik and M. Topič, "Calibration and data fusion for the miniature attitude and heading reference system", Sensors and Actuators A 138 (2007), pp. 411-420.
- [14] I. Skog and P. Händel, "Calibration of MEMS Inertial Measurement Unit" XVIII IMEK World Congress, Metrology and Sustainable Development, Rio de Janeiro, Brazil, 2006, pp. 17-22.
- [15] J. Včelak, P. Ripka, J. Kubik, A. Platil and P. Kašpar, "AMR Navigation Systems and Methods of their Calibration", Sensors and Actuators A 123-124 (2005) 122-128.
- [16] D. H. Titterton and J. L. Weston, "Strapdown Inertial Navigation Technology – 2<sup>nd</sup> Edition", Institution of Electrical Engineers, 20047
- [11] Vezzetti E., Moos S., Grivon D., Brul De Leon Rayant K., Fuentes Braco Gilmar E., Marino V., (2013), Dispositivo e Sistema di Scansione Tridimensionale e relativo metodo, Patent N°TO2013A000202
- [18] A. W. Fitzgibbon, M. Pilu and R. B. Fisher "Direct LeastSquareFitting of Ellipses", IEEE Transactions on Pattern Analysis and Machine Intelligence, Vol. 21, No. 5, May 1999.
- [19] S. Alfano and M. L. Greer, "Determining if two ellipsoids Intersect", Journal of Guidance Control and Dynamics, Vol. 26, No. 3, January-February 2003.
- [20] Rogers, D. F., and Adams, J. A., Mathematical Elements for Computer Graphics, 2nd ed., McGraw-Hill, New York, 1990, pp. 400-408.
- [21] Å. Björck, "Numerical Methods for Least Square Problems", Society of Industrial and Applied Mathematics, 1996.
- [22] S. O. H. Madwick, A. J. L. Harrison and R. Vaidyanathan, "Estimation of IMU and MARG orientation using a gradient descent algorithm", IEEE International Conference on Rehabilitation Robotics (ICORR), June 29-July 1 2011.
- [23] J. L. Marins, X. Yun, E. R. Bachmann, R. B. McGhee and Michael J. Zyda, "An Extended Kalman Filter for Quaternion-Based Orientation Estimation Using MARG Sensors", International Conference on Intelligent Robots and Systems Maui, Hawaii, USA, Oct. 29 - Nov. 03, 2001